American Journal of
Biomedical Science & Research

www.biomedgrid.com
ISSN: 2642-1747

Research Article

The Effects of Lutein: Meso-Zeaxanthin =1:2 on the Oxidative Stress-Induced Retinal Damage via Up-Regulation of MTHFD1L

Xiao Han[1†], Shuang Liu[1†], Xiaotong Zhang[2†], Sheng Zhang[1], Jinqiu Li[1], Chunmei Li[1], Yongde Hong[2], Wenzhong Wu[2], Xiang Ren[2*] and Linhua Liu[1*]

1Department of Biochemistry, College of Basic Medical Sciences, Dalian Medical University, Dalian, Liaoning 116044, China

2INNOBIO Co., Ltd., No. 49, Development Area, Dalian, 116600, China

†These authors have contributed equally to this work

***Corresponding author:** Linhua Liu and Xiang Ren, Department of Biochemistry, College of Basic Medical Sciences, Dalian Medical University, 9-Western Section, Lvshun South Road, Dalian, Liaoning 116044, P.R. China, INNOBIO Co., Ltd., No. 49, Development Area, Dalian, 116600, China.

To Cite This article: *Xiao Han, Shuang Liu, Xiaotong Zhang, Sheng Zhang, Jinqiu Li, Chunmei Li, Yongde Hong, Wenzhong Wu, Xiang Ren* and Linhua Liu*, The Effects of Lutein: Meso-Zeaxanthin =1:2 on the Oxidative Stress-Induced Retinal Damage via Up-Regulation of MTHFD1L. Am J Biomed Sci & Res. 2026 31(3) AJBSR.MS.ID.004046,* **DOI:** 10.34297/AJBSR.2026.31.004046

Received: June 09, 2026 **Published:** June 15, 2026

Abstract

Age-related Macular Degeneration (AMD) is a leading cause of irreversible blindness, driven by oxidative stress from aging, UV/blue light and genetic factors. Lutein (Lut) and zeaxanthin (MZ)-the exclusive macular carotenoids-exhibit location-specific distributions (central fovea Lut: MZ=1:2; periphery 2:1; overall macula 5:1), prompting investigation into their optimal therapeutic ratios. This study evaluates seven Lut/MZ formulations (including 5:1, 2:1, 1:1, 1:2, and 5:5:1 with 3R-3'R-zeaxanthin) in H_2O_2/blue light-stressed ARPE-19 cells and mice. The Lut: MZ=1:2 ratio demonstrated superior efficacy: it increased cell viability, reduced MDA, enhanced T-SOD and GSH-PX, and suppressed ROS in ARPE-19 cells. In vivo, this ratio upregulated MTHFD1L, activated Nrf2/HO-1 pathway, and improved serum antioxidant markers. Besides, downregulated MTHFD1L in ARPE-19 cells significantly reduces their antioxidant capacity. Ultimately, this ratio orchestrates ROS generation and exerts the best antioxidant effect by regulating the expression of MTHFD1L.

Keywords: ARPE-19; ROS; Lutein; Zeaxanthin; MTHFD1L

Introduction

Elevated levels of ROS at a heightened magnitude impair the lysosomal degradation function of ferritin, culminating in the accumulation of iron-laden ferritin within lysosomes. Consequently, iron is released into the extracellular milieu encapsulated within vesicles bounded by lysosomal membrane sealing. Fusion of these vesicles with photosensitive cells instigates iron overload, thereby compromising the viability of RPE cells [1-4]. RPE cells constitute a highly specialized monolayer of polarized pigment epithelial cells situated between the choroidal capillaries and the neural retina. It plays a pivotal role in preserving and sustaining the overlying photosensitive photoreceptors through their involvement in the formation of the outer blood-retinal barrier, as well as in the processes of phagocytosis and defense against light-induced and oxidative stress [5]. Factors such as BL exposure, elevated glucose levels, and excessive lipid content instigate a considerable increase in ROS levels within RPE cells, thereby disrupting the localized antioxidant defense system. This disruption precipitates

mitochondrial dysfunction, mitophagy, autophagic release of iron through ferritin engulfment, perturbations in lysosomal homeostasis, and inflammatory responses within RPE cells, ultimately leading to functional impairment and eventual vision loss [6-8].

Recent research has identified exposure to specific wavelengths or intensities of light as a potential cause of severe retinal damage, primarily through the induction of photomechanical, photothermal, and photochemical injuries. Photomechanical injury occurs due to a rapid escalation in energy absorbed by the RPE, leading to irreversible harm to the RPE and subsequent impairment of photoreceptors. Photothermal injury arises when the retina is briefly exposed to intense illumination, resulting in a significant elevation of tissue temperatures. In contrast, photochemical injury occurs from prolonged exposure (12-48 hours) to lower-intensity light (415-455nm), causing the deactivation of enzymes and proteins in the RPE, thereby impairing their ability to clear ROS. As the damage progresses, the closely associated photoreceptors, reliant on the RPE for nourishment and phagocytic function, become disrupted. Consequently, compromised cellular organelles in the RPE initiate the activation of apoptotic pathways, leading to the death and detachment of RPE cells. Ultimately, these processes contribute to the development of AMD [9,10].

AMD is recognized as a foremost contributor to irreversible vision impairment and blindness worldwide, presenting limited prospects for effective therapeutic interventions. In developed regions, AMD affects an estimated 20-30% of individuals aged 75 years and older [11]. Based on statistical projections, the global prevalence of AMD is on the rise due to population aging trends. It is anticipated to escalate to approximately 288 million individuals by the year 2040, with prevalence rates expected to surge to 15% by 2050. [12,13]. The progression of AMD culminates in painless central vision loss. The central alteration resides in the dysfunction of RPE cells, primarily induced by the accumulation of aging, genetic predisposition, dietary factors, smoking, and environmental influences. These factors provoke oxidative stress, ultimately resulting in central vision impairment [14-16]. There are two primary forms of AMD: dry AMD and wet AMD. Dry AMD is associated with gradual vision deterioration, characterized by thickening and structural alterations of Bruch's membrane, accumulation of lipofuscin in the nuclear membrane of RPE, and early-stage abnormal RPE morphology without pronounced symptoms. In contrast, wet AMD can precipitate sudden and severe vision loss over a short duration, potentially leading to retinal detachment and eventual blindness [17-19].

Research has demonstrated that Lut and MZ possess the ability to absorb high-energy BL within the visible light spectrum, specifically wavelengths ranging from 400 to 500nm. This absorption capability contributes to the removal of excessive Reactive Oxygen Species (ROS) within Retinal Pigment Epithelium (RPE) cells, thereby mitigating imbalances induced by oxidative stress [20-22]. Moreover, Lut plays a pivotal role in facilitating the nuclear translocation of Nuclear factor E2 related factor 2 (Nrf2), leading to its dissociation from Kelch-like ECH-associated protein 1 (Keap1). This interaction subsequently initiates the expression of a cascade of antioxidative proteins, including Glutathione Peroxidase (GSH-PX), Total Superoxide Dismutase (T-SOD), Heme Oxygenase-1 (HO-1), and Quinone Oxidoreductase 1 (NQO1), thereby enhancing resistance against oxidative stress. Simultaneously, in Hepatocellular Carcinoma (HCC), the upregulation of Methylenetetrahydrofolate Dehydrogenase 1-like Protein (MTHFD1L) aids in combating oxidative stress, with Nrf2 transcriptionally activating MTHFD1L to establish an oxidative-reductive equilibrium. MTHFD1L, a mitochondrial enzyme involved in the folate cycle, catalyzes the conversion of methylene-tetrahydrofolate into formate and Tetrahydrofolate (THF) [23].

Furthermore, specific cancer cells exhibit increased expression of MTHFD1L as a result of their heightened growth state and prolonged exposure to oxidative stress induced by metabolism. This heightened MTHFD1L expression stimulates the folate cycle, thereby enhancing DNA and protein synthesis, and bolstering antioxidative stress capabilities [24]. In HCC, Methylenetetrahydrofolate Dehydrogenase 1-like Protein (MTHFD1L) contributes to the generation and accumulation of NADPH, attaining levels sufficient to counteract oxidative stress within cancer cells [25]. Conversely, the depletion of MTHFD1L in Tongue Squamous Cell Carcinoma (TSCC) diminishes NADPH levels, thereby exacerbating ROS accumulation and hastening cellular demise under conditions of oxidative stress [26]. The role of MTHFD1L in ARPE-19 cells remains unexplored. Thus, our objective is to determine the optimal combination of Lut and MZ that exhibits the most robust resistance against oxidative stress. This study aims to investigate whether MTHFD1L participates in the antioxidative mechanisms of ARPE-19 cells and whether Lut exerts antioxidative effects by modulating MTHFD1L expression. Notably, hydrogen peroxide (H2O2) is utilized as a ROS inducer, elevating cellular ROS levels upon exposure. Therefore, both BL and H2O2 are employed in the oxidative stress model to comprehensively assess Lut's protective role against oxidative stress-induced retinal injury. Building upon this framework, our endeavor aims to advance our understanding of Lut's efficacy both in vitro and in vivo through models of retinal injury induced by oxidative stress. We aim to elucidate Lut's potential benefits in biological systems by utilizing cellular models of oxidative stress-induced retinal injury alongside a murine model.

Materials and Methods

Experimental Material

The Human Retinal Pigment Epithelia (ARPE-19) cell line is obtained from Hunan Haixing Biotechnology Co., Ltd. ARPE-19 cells are cultured in Dulbecco's modified Eagle's medium/nutrient mixture F-12 (DMEM/F12; WELGENE, Gyeongsan, Korea) containing 10% FBS (ExCell Bio, Lnc.) and 1% penicillin/streptomycin antibiotic (Seven Biotech) at 37°C with 5% CO2.

Both lutein and zeaxanthin used in this paper were provided by INNOBIO® Co., Inc. Dalian, China.

Model of Lut Pretreatment of ARPE-19 Cells Against Oxidative Stress Damage

ARPE-19 cells are seeded at a density of 1.5×105 cells in 6-well culture plates and treated with or without lutein (20μmol/L) for 24 hours. Subsequently, the cells are washed with Phosphate-Buffered Saline (PBS) and supplemented with complete medium. The ARPE-19 cells are then exposed to blue light with a light intensity ranging from 4000 to 5333 Lux for 2 hours or treated with hydrogen peroxide (H2O2) at a concentration of 0.3mM for 4 hours.

In vivo animal model: This protocol of the animal experiment is approved by the Experimental Animal Ethics Committee, Dalian Medical University (Ethic number: AEE21112). Twenty-five male KM mice had a body weight ranging from 28g to 32g are obtained from Liaoning Changsheng Biotechnology Co., LTD. All the mice were allowed free access to food and water. During grouping, a completely randomized grouping methods was employed. The experimental animals were numbered from 1 to 25, and Excel software was used to generate random numbers for sorting and assigning the groups. By randomizing both cage palcement and measurement order, potential confouding factors are minimized, leading to more reliable and valid experimental results. Each mouse received a gavage (1mL per mouse) daily at 8:00 AM for 14 consecutive days. The specific grouping and experimental details are as follows: Prior to Blue Light (BL) treatment, 2 of the 5 groups receive physiological saline treatment, serving as the blank Control (Ctrl) group and the oxidative stress model (BL) group, respectively. Others are treated with Lut, MZ and Lut: MZ=20mg/kg. Following drug administration, the Ctrl group is kept in darkness for 12 hours, while the other 4 subgroups are exposed to BL with a light intensity ranging from 4000 to 5333 Lux for 12 hours. Then, all mice were euthanized by intraperitoneal injection of an overdose of sodium pentobarbital, and all the eyeballs and blood from each mouse were collected for subsequent experiments..

Cell counting kit-8 (CCK-8) assay

Cell viability is assessed using the cell counting kit-8 (CCK-8) assay (Seven Biotech.), following the manufacturer's protocol. Prior to the CCK-8 experiment, ARPE-19 cells are treated with or without Lut and exposed to BL. Subsequently, these ARPE-19 cells are seeded in 96-well culture plates at a density of 6×103 cells per well. Following incubation with the CCK-8 solution at 37°C for 4 hours, cell viability is measured at an absorbance of 450 nm using a microplate reader (Tecan, Infinite F50, Swiss).

Glutathione peroxidase (GSH-PX) assay

Preparation of reagents is performed according to the instructions provided by the GSH-PX kit (NanJingJianCheng Bio Lnc.). In the enzymatic reaction, reagent application solution is sequentially added, and serum is diluted (animal serum:saline =1:4) and thoroughly mixed. The mixture is then centrifuged at 3500~4000 rpm for 10 minutes, and 1mL of the supernatant is used for color reaction. For the color development reaction, reagent application liquid and top cleaning liquid are added sequentially. After thorough mixing, the mixture is left at room temperature for 15 minutes. The supernatant is collected, and the absorbance is measured at 412nm. The activity of GSH-PX is calculated using the provided formula.

Determination of total superoxide dismutase (T-SOD)

Reagent preparation follows the instructions provided by the T-SOD kit (NanJingJianCheng Bio Lnc.). Serum is diluted (animal serum:saline =1:4) and thoroughly mixed with reagents. The mixture is then incubated at a constant temperature of 37°C for 40 minutes, followed by the addition of coloring liquid solution. After thorough mixing, the mixture is allowed to stand at room temperature for 10 minutes. Absorbance is measured at 550 nm, and SOD activity is calculated using the provided formula.

Determination of malondialdehyde (MDA)

Reagents are prepared according to the instructions provided by the MDA kit (NanJingJianCheng Bio Lnc.). The procedure involves sequential addition of reagent application solution, anhydrous ethanol, diluted serum (animal serum:saline =1:4), and 50% glacial acetic acid, with thorough mixing after each addition. The mixture is then incubated for 40 minutes in a 95°C water bath, followed by cooling with flowing water. Subsequently, samples are centrifuged at 3500~4000 rpm for 10 minutes, and the supernatant is collected. Absorbance is measured at 532 nm to determine the level of MDA, which is calculated using the provided formula.

Hematoxylin-Eosin stain Extraction and fixation

After euthanasia, both ocular tissues were immediately excised and fixed with 4% paraformaldehyde overnight at room temperature, dehydrated in a graded ethanol series, and embedded inparaffin. Sections were made along the optic nerve of the eyeball using a rotary slicing machine, Sagittal sections containing the whole retina were cut 5μm thick for H&E. The tissue sections are subjected to a 40-46°C water bath, mounted on slides, and dried at 60°C for 2 hours. H&E staining was performed, and the mean Outer Nuclear Layer (ONL) thickness was measured at 140μm (left/right) from the retinal nerve center using the Axio Vision SE644 (ZEISS) program. After measuring the thickness of ONL in the opposite eyeball in a similar manner, the average value was used as the final ONL thickness.

Western Blot

Cells and retinal tissues are collected and lysed using lysis buffer with proteinase inhibitor to extract the total protein and protein concentration is measured using the BCA protein assay. Protein lysates are separated by 4-15% SDS-PAGE and transfer to the PVDF membrane (0.22μM aperture). Next, all these membranes

are blocked using 5% skim milk and incubated with the primary antibodies (Proteintech Group, Inc.) including MTHFD1L, Nrf2, HO-1and β-Actin overnight at 4°C. Afterward, the secondary antibody (goat antirabbit and goat antimouse) IgG/HRP is incubated to membranes for 1 hour at room temperature.

ROS Assay

ARPE-19 cells are seeded in 6-well culture plate (1.5× 105 cells) and treated with or without Lut and BL. In-situ loading probe: DCFH-DA is prepared with a serum-free medium, with a final concentration of 10 μmol/L, 1mL per dish, incubated in a cell incubator at 37°C for 20 minutes, and washed three times with PBS. Then, cells are harvested and centrifuged at a speed of 1000g for 3minutes. Remove the supernatant, add 1mL cold PBS to suspend cells, and then repeat centrifugal precipitation. Flow cytometry detects 485 nm stimulated wavelength and 525nm emission wavelength.

Cell Transfection

Cell transfection is performed using reagent (Golden Trans Technology, ChangChun, China.) following the guideline provided by the manufacture. Sequences in this research were shown as below: MTHFD1L-Homo-658 (sense: 5'-GGAUGGAGUAACAGACAUATT-3' and antisense:5'-UAUGUCUGUUACUCCAUCCTT-3'). After cells are initially transfected for 6 hours, cell culture medium is replaced with DMEM/ F12 medium containing 10% FBS and 1% penicillin/ streptomycin antibiotic and then cells are incubated for 24 hours to be collected for the following experiments.

Results

The Lut MZ=1:2 treatment group exhibited a significantly enhanced cellular viability of ARPE-19 cells during the process of BL damage in comparison to the other treatment groups

To investigate the impact of varying ratios of Lut and MZ on the vitality of ARPE-19 cells under BL damage, distinct treatments are administered, including Lut, MZ, Lut: MZ=5:1, Lut: MZ=2:1, Lut: MZ=1:1, Lut: MZ=1:2 and Lut:MZ:3R-3'R-zeaxanthin =5:5:1 (Lut at 20 μmol/L). Following a 24-hour incubation, with the exception of the control (Ctrl) group, all other groups are subjected to 2 hours of BL exposure at intensities ranging from 4000 to 5333 Lux. The cellular viability alterations resulting from the various Lut and MZ pre-treatments are evaluated utilizing CCK-8 assays. The outcomes substantiate the successful establishment of the BL-induced model, as evidenced by a substantial reduction in cellular viability in the BL-exposed group in comparison to the Ctrl group. Based on rigorous statistical analyses, it is demonstrated that the cellular viability of all Lut: MZ pre-treatment groups, with different ratios, significantly increased in contrast to the BL-exposed group. Particularly noteworthy is the pronounced divergence observed between the Lut: MZ =1:2 treatment group and the other Lut and MZ treatment groups, underscoring the distinctive augmentation of cellular viability against BL-induced damage in the Lut: MZ =1:2 combination. This compellingly illustrates that Lut: MZ =1:2 exhibits a significantly amplified effect on enhancing cellular viability of ARPE-19 cells under BL injury compared to other Lut and MZ ratios (Figure 1).

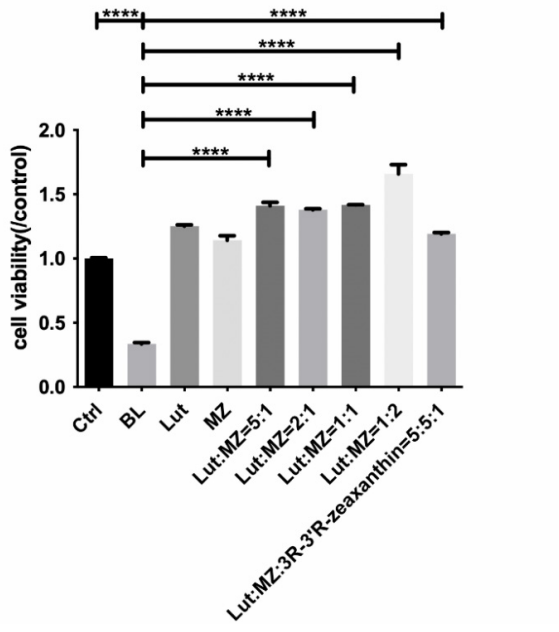

Figure 1: Cellular viability of ARPE-19 cells during the BL damage process following pre-treatment with varying ratios of Lut and MZ. Cellular viability is assessed using the CCK-8 assay. Experimental data are subjected to analysis using GraphPad Prism 9 software, leading to the generation of graphical representations. The statistical evaluation involved the execution of three independent replicates to facilitate robust statistical analysis. ****P<0.0001, **P<0.01, *P<0.05.

The Lut MZ =1:2 treatment group exhibited a pronounced enhancement in the activities of GSH-PX and T-SOD in ARPE-19 cells during the process of BL damage and demonstrated a reduction in MDA levels in comparison to the other treatment groups

Subsequently, we employed GSH-PX, T-SOD, and MDA assay kits to investigate the variations in antioxidative stress among cells pre-treated with different ratios of Lut and MZ. After a 24-hour incubation period with distinct treatments including Lut, MZ, Lut: MZ=5:1, Lut: MZ=2:1, Lut: MZ=1:1, Lut: MZ=1:2 and Lut:MZ:3R-3'R-zeaxanthin =5:5:1, all groups, excluding the Ctrl group, are exposed to 2 hours of BL at intensities ranging from 4000 to 5333 Lux. The results demonstrate a considerable reduction in GSH-PX and T-SOD levels and a notable elevation in MDA content in the BL-exposed group compared to the Ctrl group, substantiating the successful establishment of the BL-induced model. Based on meticulous statistical analyses, all Lut: MZ treatment groups with different ratios exhibited a significant augmentation in cellular GSH-PX and T-SOD activities compared to the BL-exposed group (Figure 2A, B). Additionally, these treatment groups demonstrated a reduction in MDA levels (Figure 2C). Specifically, the Lut: MZ =1:2 treatment group displayed a discernible disparity in GSH-PX levels from other Lut and MZ treatment groups, affirming the distinctive enhancement in cellular GSH-PX and T-SOD activities, meanwhile diminished MDA levels, attributed to Lut: MZ =1:2 (Figure 2).

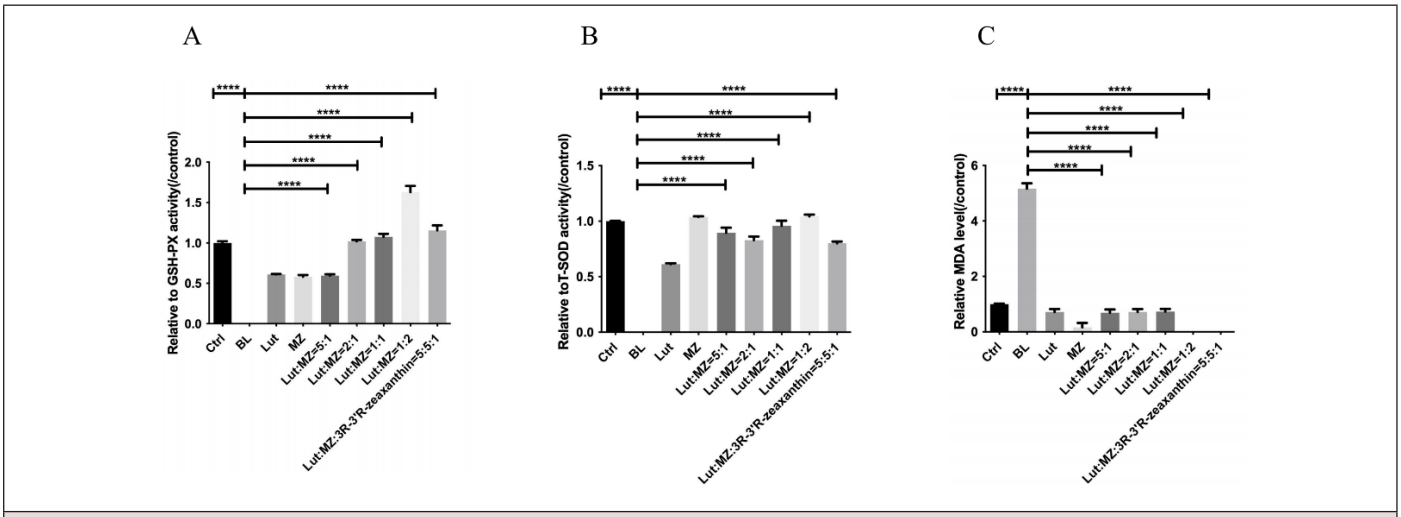

Figure 2: GSH-PX, T-SOD, and MDA levels in ARPE-19 cells during the BL damage process following pre-treatment with varying ratios of Lut and MZ. (A) cellular GSH-PX activity are evaluated using the GSH-PX assay kit. (B) T-SOD activity in cells is assessed using the T-SOD assay kit. (C) cellular MDA levels are measured utilizing the MDA assay kit. Experimental data are subjected to analysis using GraphPad Prism 9 software, leading to the generation of graphical representations. The statistical evaluation encompassed the execution of three independent replicates to facilitate robust statistical analysis.

The Lut MZ =1:2 treatment group exhibited a significant reduction in ROS of ARPE-19 cells during the H_2O_2 -induced damage

Given our previous findings that Lut: MZ=1:2 demonstrated the fantastic ratio for mitigating BL-induced damage, it becomes pertinent to ascertain whether the same combination holds efficacy in countering oxidative stress and protecting ARPE-19 cells against H2O2-induced injury. This prompts us to delve into the mechanistic insights of the protective effects of different Lut: MZ ratios in pre-treated ARPE-19 cells against H_2O_2 damage. For this purpose, we conducted assessments of ROS levels in ARPE-19 cells subjected to H_2O_2 damage under various Lut: MZ pre-treatment conditions, including Lut, MZ, Lut: MZ=5:1, Lut: MZ=2:1, Lut: MZ=1:1, Lut: MZ=1:2, and Lut:MZ:3R,3'R-zeaxanthin=5:5:1. After a 24-hour pre-treatment, ARPE-19 cells are exposed to H_2O_2 for 4 hours to induce oxidative stress, excluding the Ctrl group. Utilizing flow cytometry and DCFH-DA staining for ROS detection, the results revealed a significant elevation of ROS levels in the H2O2-induced group compared to the Ctrl, confirming the success of the H2O2-induced model. Notably, through statistical analysis, all Lut: MZ-treated groups exhibited a notable reduction in cellular ROS levels when compared to the H2O2 group. Among them, the Lut: MZ =1:2 treatment group exhibited the lowest ROS content (Figure 3).

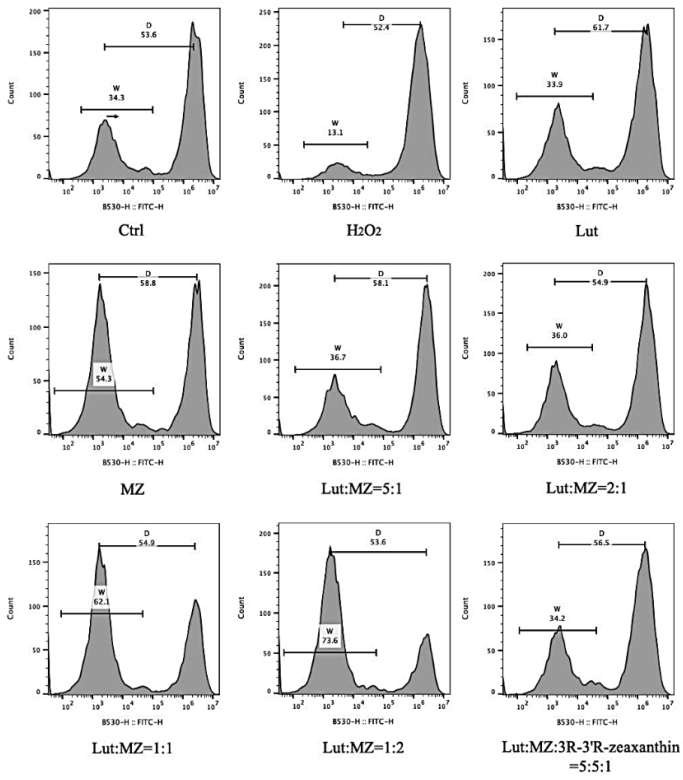

Group	Ctrl	H_2O_2	Lut	MZ	Lut:MZ= 5:1	Lut:MZ= 2:1	Lut:MZ= 1:1	Lut:MZ= 1:2	Lut:MZ:3R-3'R-zeaxanthin= 5:5:1
D/W	1.56	4.0	1.82	1.08	1.58	1.52	0.88	0.73	1.65

Figure 3: ROS Levels in ARPE-19 cells during H_2O_2-induced injury following pre-treatment with different Lut and MZ Ratios. ROS levels are assessed using flow cytometry, and the results are processed and graphed using FlowJo software.

The Lut: MZ =1:2 treatment group exhibited a significant enhancement in the activities of GSH-PX and T-SOD in mouse serum during the BL damage, in contrast to the other treatment groups and demonstrated a reduction in MDA levels

To further explore the impact of different ratios of Lut: MZ pre-treatment groups in the murine biological system, animal models are established. After a fourteen-day administration of Lut, MZ, and Lut: MZ =1:2 to mice, excluding the Ctrl group, all groups are subjected to 12 hours of BL exposure at intensities ranging from 4000 to 5333 Lux. Utilizing respective assay kits for GSH-PX, MDA, and SOD. The assessment is performed post-BL exposure. The results revealed that subsequent to BL exposure, the levels of MDA in the serum of the BL-exposed group of mice are significantly elevated compared to those in the serum of the Ctrl group. Furthermore, the activities of GSH-PX and SOD in the serum of the BL-exposed group of mice are notably reduced in comparison to those in the serum of the Ctrl group, confirming the successful establishment of the BL-induced model. Based on rigorous statistical analyses, all Lut: MZ pre-treatment groups with varying ratios significantly reduced MDA levels compared to the BL-exposed group (Figure 4C) and significantly enhanced GSH-PX and SOD activities (Figure 4A, B). Notably, the Lut: MZ =1:2 treatment group demonstrated significant disparities in MDA levels, as well as GSH-PX and SOD activities, in comparison to both the Lut and MZ treatment groups of mice (Figure 4).

The Lut: MZ =1:2 treatment group exhibited a substantial augmentation, as compared to the other treatment groups, in the thickness of the Inner Nuclear Layer (INL) and Outer Nuclear Layer (ONL) and demonstrated a heightened expression levels of MTHFD1L, Nrf2 and HO-1 in the retinas of mice subjected to BL damage

After administering Lut, MZ, and Lut: MZ =1:2 to mice for a duration of 14 days, with the exception of the Control (Ctrl) group, all other groups are subjected to 12 hours of BL exposure ranging from 4000 to 5333 Lux. Subsequently, mouse eyeball sections are obtained, and Hematoxylin and Eosin (H&E) staining is employed to examine retinal changes in response to Lut: MZ =1:2 against BL-induced damage. The results indicated that following BL exposure, the thickness of the INL and ONL in mouse eyeballs reduced, accompanied by irregular arrangement. Post-administration of the compounds, there is an observed thickening of INL and ONL layers in mouse eyeballs, with a regular arrangement. Remarkably, the Lut: MZ =1:2 group showed a restoration of thickness levels similar to the Ctrl group (Figure 5A). Based on histological analysis, we measured ONL thickness to confirm the degree of

retinal degeneration. The thickness of the ONL was significantly lower in BL group than in Ctrl group. Administration of Lut:MZ =1:2 alleviated the degeneration of the retinal layer (Figure 5B). Furthermore, Western Blot analysis is conducted to monitor the expression of Nrf2, HO-1, and MTHFD1L in retinal tissues. The results showed that this protein expression was downregulated by BL-exposure, meanwhile this protein expression was upregulated by pre-treatment of Lut, MZ and Lut: MZ =1:2 significantly. (Figure 5C).

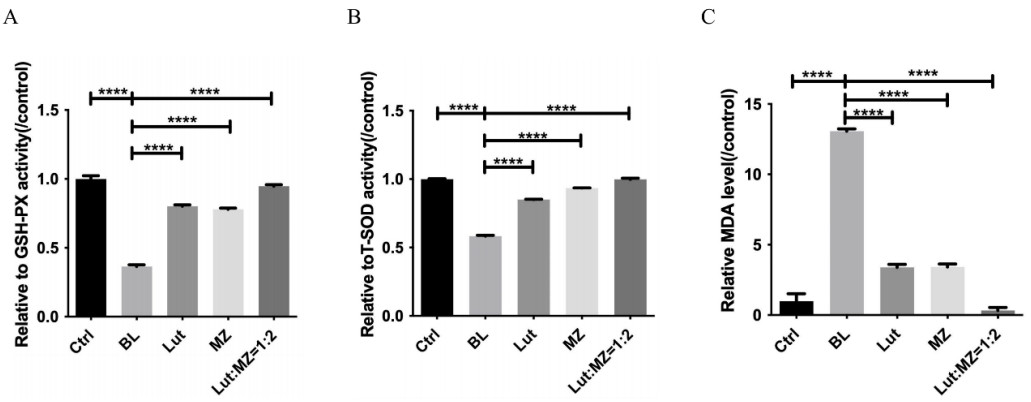

Figure 4: MDA levels, T-SOD, and GSH-PX activities in the murine's serum during the BL damage process. (A) GSH-PX activity in serum are assessed using the GSH-PX assay kit. (B) T-SOD activity in the serum is evaluated using the T-SOD assay kit. (C) Variations in serum MDA levels are measured utilizing the MDA assay kit. Experimental data are subjected to analysis using GraphPad Prism 9 software, involving three independent replicates to facilitate robust statistical analysis. ****P<0.0001.

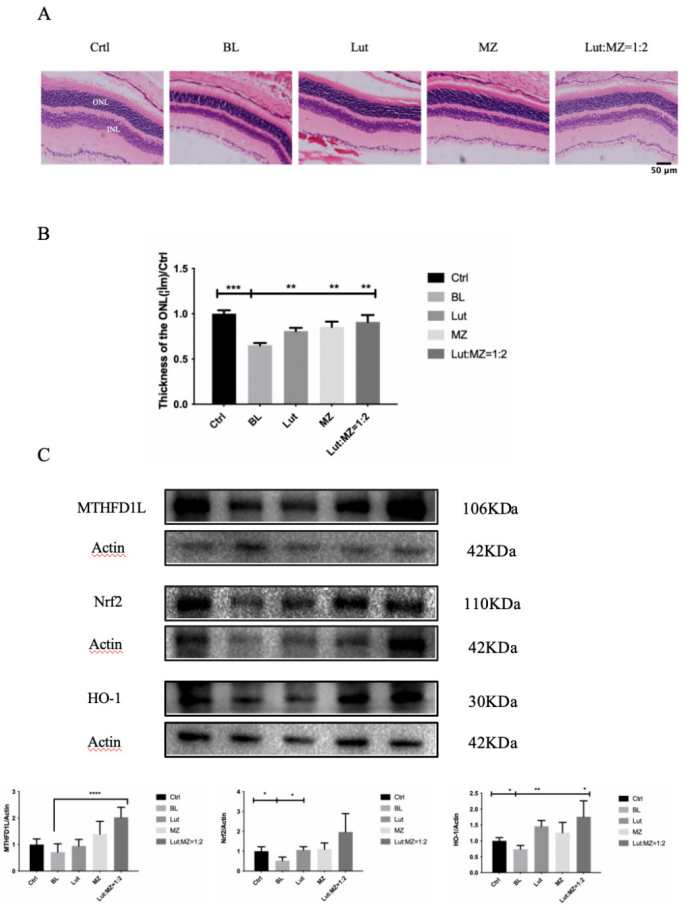

Figure 5: (A) Retinal alterations in mice during the BL damage process following pre-treatment with combined Lut and MZ formulations compared to individual Lut and MZ pre-treatments. (ONL: Outer Nuclear Layer, INL: Inner Nuclear Layer. Graphical representation is generated using ImageJ software.) (B) Measurement of the ONL thickness, Scale bar = 50μm. The results are analyzed using GraphPad Prism9. (C) Protein expression levels of MTHFD1L, Nrf2, and HO-1 in murine retinas are evaluated using WB analysis. WB results are subjected to analysis using GraphPad Prism 9 software, and graphical representations are generated. The experiments are repeated three times for robust statistical analysis. ****P<0.0001, ***P<0.001, **P<0.01, *P<0.05.

The Lut: MZ=1:2 treatment group significantly upregulated the expression of MTHFD1L in the cells. Subsequently, ARPE-19 cells with suppressed MTHFD1L expression are established

Previous findings indicate that the expression level of MTHFD1L is modulated by Lut: MZ=1:2 treatment during BL-induced retina damage. To elucidate the functional role of MTHFD1L in oxidative stress-induced retina damage, ARPE-19 cells are treated with Lut: MZ=1:2, and the expression level of MTHFD1L protein is assessed via Western blot (WB) analysis. Statistical analysis reveals a significant increase in MTHFD1L expression in the Lut: MZ=1:2 treatment group compared to the Ctrl group (Figure 6A), indicating a marked elevation in MTHFD1L expression in ARPE-19 cells treated with Lut: MZ=1:2. Subsequently, ARPE-19 cells with suppressed MTHFD1L expression are established through siRNA construction. Protein levels are examined using WB analysis to confirm the successful knockdown of MTHFD1L. The results conclusively demonstrate that MTHFD1L is effectively downregulated by siRNA at the protein level (Figure 6B).

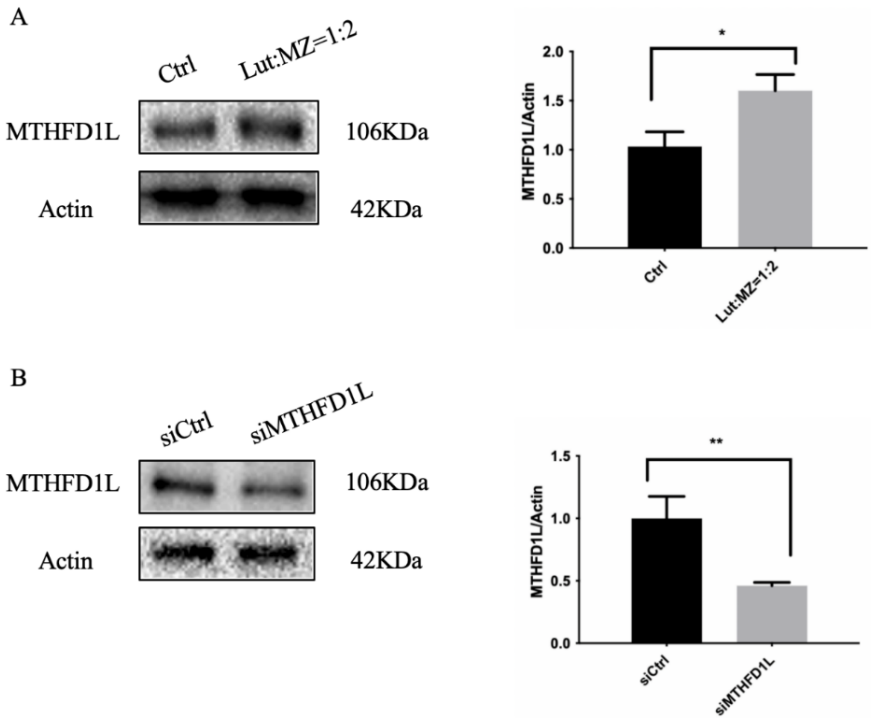

Figure 6: (A) Expression levels of MTHFD1L after Lut: MZ=1:2 pretreatment in ARPE-19 cells assessed by WB analysis. (B) Expression levels of MTHFD1L in ARPE-19 cells with MTHFD1L knockdown examined by WB analysis. Graphical representations are generated using ImageJ software. The results of the Western blot experiments are analyzed using GraphPad Prism 6 software and presented in graphical format. The experiments are conducted in triplicate and subjected to statistical analysis. **P<0.01 , *P<0.05.

Knocking down MTHFD1L significantly decreased the cell viability of the Lut: MZ=1:2-treated group

Investigating the effect of MTHFD1L knockdown on cell viability in ARPE-19 cells, following siRNA transfection, CCK-8 assays are employed to explore the relationship between Lut: MZ=1:2 resistance to BL-induced oxidative stress and MTHFD1L expression level. The results are quantified using OD values. Statistical analysis revealed that the cell viability of the BL group significantly decreased compared to the Ctrl group. The siMTHFD1L+BL group exhibited a significant decrease in cell viability compared to the siMTHFD1L group. Conversely, the Lut: MZ=1:2+BL group demonstrated a significant increase in cell viability compared to the BL group. Moreover, the siMTHFD1L+Lut:MZ=1:2+BL group displayed a significant increase in cell viability compared to the siMTHFD1L+BL group. The cell viability of the siMTHFD1L group and siMTHFD1L+Lut:MZ=1:2 group significantly decreased compared to the Ctrl and Lut: MZ=1:2 groups, respectively. Furthermore, the siMTHFD1L+Lut:MZ=1:2+BL group exhibited a significant decrease in cell viability compared to the Lut: MZ=1:2+BL group. Collectively, all MTHFD1L knockdown groups exhibited a notable reduction in cell viability compared to their respective non-knockdown counterparts. Therefore, Lut: MZ=1:2 could effectively restore cell viability, but the knockdown of MTHFD1L significantly inhibited its effect, indicating that Lut: MZ=1:2 played a protective role by regulating MTHFD1L (Figure 7).

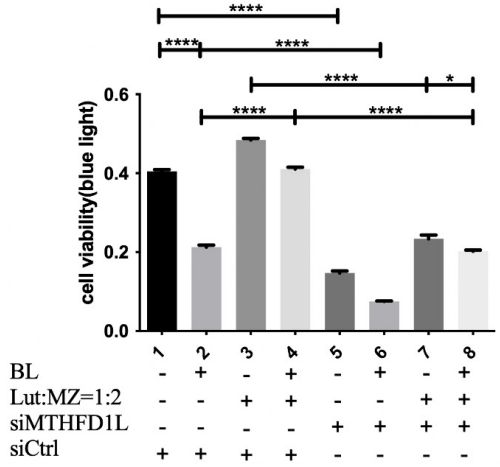

Figure 7: Cell viability of ARPE-19 cells during BL-induced injury following MTHFD1L gene knockdown and Lut: MZ=1:2 pretreatment. Experimental results are analyzed and graphed using GraphPad Prism 6. Three independent replicate experiments are conducted for statistical analysis. ****P<0.0001, ***P<0.0005, *P<0.05.

Knocking down MTHFD1L significantly increased the levels of ROS in ARPE-19 cells subjected to H_2O_2-induced injury, following pretreatment with Lut: MZ=1:2

To investigate the underlying mechanisms of MTHFD1L's protective role in ARPE-19 cells against H_2O_2-induced injury under Lut: MZ=1:2 pretreatment, post siRNA transfection, we treated ARPE-19 cells with Lut: MZ=1:2 for 24 hours, followed by exposure to 300μmol/L H_2O_2 for 4 hours to induce oxidative stress. Using flow cytometry and DCFH-DA staining, we measured cellular levels of ROS. The results revealed that the ROS content in the H_2O_2 treated model group is significantly higher compared to the Ctrl group, confirming the success of H_2O_2-induced modeling. The Lut: MZ=1:2-treated group exhibited a significant reduction in cellular ROS levels compared to the H_2O_2-treated group. The ROS levels in the H_2O_2+ Lut: MZ=1:2-treated group nearly returned to Ctrl group levels. In contrast, the siMTHFD1L group showed a significant increase in ROS compared to the Ctrl group. Similarly, the siMTHFD1L+H_2O_2 group demonstrated a notable elevation in ROS content compared to the H_2O_2 group. This indicates the antioxidative role of MTHFD1L in ARPE-19 cells. Interestingly, the siMTHFD1L+Lut:MZ=1:2 group exhibited a significant rise in ROS content compared to the Lut: MZ=1:2 group. Likewise, the siMTHFD1L+H_2O_2+ Lut: MZ=1:2 group demonstrated a noticeable increase in ROS levels compared to the H_2O_2+ Lut: MZ=1:2 group, suggesting that the reduction in MTHFD1L weakened the ROS scavenging effect of Lut: MZ=1:2 on ARPE-19 cells (Figure 8).

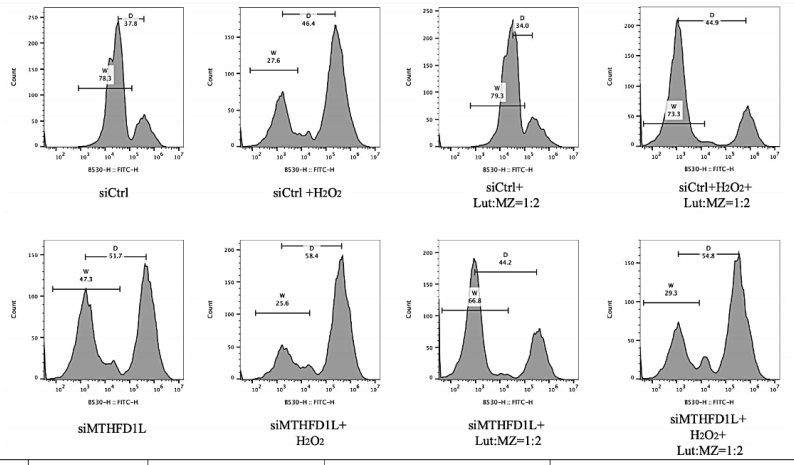

Group	siCtrl	H_2O_2	Lut:MZ=1:2	H_2O_2+Lut:MZ=1:2
D/W	0.47	1.51	0.46	0.58
Group	siMTHFD1L	siMTHFD1L+H_2O_2	siMTHFD1L+Lut:MZ=1:2	siMTHFD1L+H_2O_2+Lut:MZ=1:2
D/W	1.07	2.4	0.64	1.8

Figure 8: ROS levels in ARPE-19 cells during H_2O_2-induced injury after knockdown of MTHFD1L gene and Lut: MZ=1:2 pretreatment. ROS levels are assessed using flow cytometry, and the results are analyzed and graphed using FlowJo software.

Discussion

Age-related Macular Degeneration (AMD) is a progressive disease characterized by irreversible vision loss. Statistics indicate that the overall prevalence of AMD among individuals aged 50 and above in developed countries is approximately 11%, with 2% attributed to wet AMD. Clinical management and prognosis of AMD present considerable challenges. In China, the aging population and growing public concern for eye health have paralleled rapid economic development. Nevertheless, the task of preventing blindness due to AMD remains formidable. Currently, specific drugs for treating AMD are lacking in the market, and management primarily revolves around antioxidant medications and laser surgery [27]. Lut is one of the important carotenoids, which is orange-yellow in color and in the form of powder. Its physical properties are insoluble in water, soluble in organic solvents, readily oxidized denaturation and difficult to preserve [28]. Lut and MZ co-exist in nature, which are the main components of plant pigments such as corn and vegetables. They are contained in chloroplasts and have a protective effect on photooxidation, photodestruction and photothermal damage. They are the main pigments in the macular area of human retina. It can resist cell and organ damage caused by oxygen radicals in the human body, and prevent AMD and other symptoms caused by aging [29, 30]. The severity of AMD in patients is clinically diagnosed using Macular Pigment Optical Density (MPOD). MPOD serves as a visual parameter for assessing the content of Lut and Z in the macular region of the retina. The highest concentrations of Lut and Z are found at the center of the macular region, with their concentrations gradually decreasing as distance from the center increases. MPOD shows a positive correlation with dietary and serum levels of Lut and a negative correlation with systemic oxidative stress [31]. Detection of Lut and Z in blood, macular pigment, and skin provides valuable information for treating AMD, enhancing prognosis, and follow-up assessments. As technological advancements continue, a deeper understanding of the molecular mechanisms underlying AMD onset contributes to refining treatment strategies for AMD [32].

The major pigments present in the macular region of the retina include Lut and Z. However, the distribution and ratio of Lut and Z in the retina vary. While the total ratio of Lut to Z in the entire retina is 5:1, the central macular region exhibits a Lut to Z ratio of less than 1:2 [33]. Research indicates that Lut and Z are distributed in different proportions in the macular area [34]. Consequently, we hypothesized that combinations of Lut and MZ in different ratios could impact their biological activities against oxidative stress induced retina damage. Thus, we designed various combinations of Lut and MZ in different ratios: Lut, MZ, Lut: MZ=5:1, Lut: MZ=2:1, Lut: MZ=1:1, Lut: MZ=1:2, and Lut:MZ:3R, 3'R-zeaxanthin=5:5:1 for investigation. In this study, we pre-treated ARPE-19 cells with Lut and then exposed them to BL with an average illumination of 4000~5333 lux for 2 hours. We conducted CCK-8 experiments to assess the effect of various Lut and MZ combinations on ARPE-19 cell viability. The results indicated that Lut: MZ=1:2 significantly enhanced the cell viability of ARPE-19 cells after BL injury (Figure 1). Subsequently, we measured the activity of GSH-PX and T-SOD as well as the level of MDA in ARPE-19 cells. The findings demonstrated that Lut: MZ=1:2 markedly increased the activity of GSH-PX and T-SOD while reducing the level of MDA in the cells (Figure 2). Currently, the most commonly used ratio of Lut to MZ in nutritional supplements and drugs for research and clinical treatment of AMD is 5:1. In this study, we discovered that increasing the proportion of MZ in Lut and MZ complexes significantly enhanced their protective effects against BL-induced damage in ARPE-19 cells. Ultimately, we identified Lut: MZ=1:2 as the most effective combination for resisting BL damage and, concurrently, as the optimal ratio for countering H2O2-induced damage (Figure 3). Lut: MZ=1:2 holds promise as a novel and more efficient antioxidant product, paving the way for further exploration into its molecular mechanisms.

In order to further elucidate the molecular mechanisms underlying the protective effects of Lut: MZ=1:2 against oxidative stress in ARPE-19 cells, we employed assay kits to assess the expression of antioxidant enzymes in a Lut: MZ=1:2 pre-treated BL injury mouse model. The results demonstrated a significant enhancement of GSH-PX and T-SOD activities, accompanied by a substantial reduction in MDA levels upon Lut: MZ=1:2 pretreatment (Figure 4). Through H&E staining, we observed changes in the retinal tissue of BL-injured mice: the thickness and arrangement of the inner nuclear layer (INL) and outer nuclear layer (ONL) in mouse eyeballs became irregular and thinner. However, pretreatment with Lut: MZ=1:2 resulted in increased thickness and more orderly arrangement of INL and ONL (Figure 5A). In recent years, research has revealed that Lut not only protects the retina by absorbing BL but also influences antioxidant signaling pathways. Specifically, Lut is involved in the Keap1/Nrf2/ARE pathway to counteract oxidative stress-induced retinal damage. Elevated levels of ROS trigger the dissociation of Nrf2 from Keap1, causing its translocation to the cell nucleus, where it binds to downstream Antioxidant Response Elements (ARE). This activation leads to the transcription of numerous antioxidant enzymes, including HO-1 and NQO1, alleviating oxidative stress-induced cellular redox imbalance [35].

Furthermore, Nrf2 transcribes and activates MTHFD1L, promoting folate cycling, enhancing DNA and amino acid synthesis, and consequently bolstering cellular resistance against high ROS levels in HCC [36]. While there are reports of the anti-oxidative role of the MTHFD1L gene in cancer, its function in the anti-oxidative process of ARPE-19 cells remains unexplored. In this study, Western blot results revealed a significant increase in the expression of Nrf2, HO-1, and MTHFD1L in mouse retinal tissues of the Lut: MZ=1:2-treated group (Figure 5B). Additionally, the Lut: MZ=1:2-treated group exhibited significantly elevated expression levels of MTHFD1L in ARPE-19 cells (Figure 6A). Subsequently, we established MTHFD1L-knockdown ARPE-19 cells (Figure 6B). CCK-8 assay results indicated that the cell viability of Lut: MZ=1:2 pre-treated BL-injured ARPE-19 cells is notably reduced upon

MTHFD1L knockdown (Figure 7). Moreover, MTHFD1L knockdown led to a significant increase in ROS levels upon H2O2-induced damage (Figure 8). These findings collectively suggest that Lut: MZ=1:2 can decrease the ROS levels by up-regulating MTHFD1L in ARPE-19 cells, thereby safeguarding the retina from oxidative stress-induced damage.

In this study, we employed both BL and H_2O_2-induced oxidative stress to investigate the protective effects of Lut: MZ=1:2 on the Retinal Pigment Epithelium (RPE). Our results demonstrate that Lut: MZ=1:2 effectively safeguards the RPE from oxidative stress-induced damage by regulating the expression of MTHFD1L and inhibiting the production of ROS. These findings suggest that MTHFD1L represents a promising therapeutic target for mitigating oxidative stress-induced damage in retinal epithelial cells. However, the precise regulatory mechanism of Lut on MTHFD1L remains incompletely understood. Further research is warranted to elucidate these intricate mechanisms and provide a comprehensive understanding. Such efforts are expected to contribute to the development of effective lutein-based products and offer valuable theoretical insights and directions for the treatment of AMD.

Conclusions

The combination of Lut and MZ in a 1:2 ratio demonstrates superior resilience against oxidative stress compared to other combinations. Furthermore, this specific combination significantly enhances the expression of MTHFD1L. Upon suppression of MTHFD1L expression, the protective effect of the 1:2 Lut to MZ combination against oxidative stress-induced retinal damage is notably diminished. These findings preliminarily suggest that the 1:2 Lut to MZ combination may exert its effects on oxidative stress-induced retinal damage by modulating MTHFD1L.

Data Availability Statement

The data are contained within this article.

Conflicts of Interest

The authors declare that they have no competing interests.

Acknowledgements

This study was supported by grants from the project of the Department of Education of Liaoning province (Grant No: 5061099).

Funding

There was no funding for this study.

Authors' Contributions

Xiao Han: Investigation

Shuang Liu: Writing - original draft

Xiaotong Zhang: Data curation

Sheng Zhang: Conceptualization

Jinqiu Li: Resources

Chunmei Li: Funding acquisition

Yongde Hong: Validation

Wenzhong Wu: Funding acquisition

Xiang Ren: Supervision

Linhua Liu: Supervision, Writing - review and editing

Ethics Approval and Consent to Participate

This protocol of the animal experiment is approved by the Experimental Animal Ethics Committee, Dalian Medical University (Ethic number: AEE21112). Twenty-five male KM mice had a body weight ranging from 28g to 32g are obtained from Liaoning Changsheng Biotechnology Co., LTD.

Patient Consent for Publication

Not applicable.

References

1. Ashok A, Chaudhary S, Wise AS, Rana NA, McDonald D, et al. (2021) Release of Iron-Loaded Ferritin in Sodium Iodate-Induced Model of Age-Related Macular Degeneration: An In-Vitro and In-Vivo Study. Antioxidants (Basel, Switzerland) 10(8): 1253.
2. Forrester SJ, Kikuchi DS, Hernandes MS, Xu Q, Griendling KK (2018) Reactive Oxygen Species in Metabolic and Inflammatory Signaling. Circulation research 122(6): 877-902.
3. Bian Q, Gao S, Zhou J, Qin J, Taylor A, et al. (2012) Lutein and zeaxanthin supplementation reduces photooxidative damage and modulates the expression of inflammation-related genes in retinal pigment epithelial cells. Free radical biology & medicine 53(6): 1298-1307.
4. Mrowicka M, Mrowicki J, Kucharska E, Majsterek I (2022) Lutein and Zeaxanthin and Their Roles in Age-Related Macular Degeneration-neurodegenerative disease. Nutrients 14(4): 827.
5. Intartaglia D, Giamundo G, Conte I (2022) Autophagy in the retinal pigment epithelium: a new vision and future challenges. The FEBS journal. 289(22): 7199-7212.
6. Bhattarai N, Korhonen E, Mysore Y, Kaarniranta K, Kauppinen A (2021) Hydroquinone Induces NLRP3-Independent IL-18 Release from ARPE-19 Cells. Cells 10(6):1405.
7. Zhang Y, Xi X, Mei Y, Zhao X, Zhou L, et al. (2019) High-glucose induces retinal pigment epithelium mitochondrial pathways of apoptosis and inhibits mitophagy by regulating ROS/PINK1/Parkin signal pathway. Biomedecine & pharmacotherapie 111: 1315-1325.
8. Chen L, Ma B, Liu X, Hao Y, Yang X, et al. (2020) H_2O_2 induces oxidative stress damage through the BMP-6/SMAD/hepcidin axis. Development, growth & differentiation 62(2): 139-146.
9. Ma H, Yang F, Ding XQ (2022) Deficiency of thyroid hormone receptor protects retinal pigment epithelium and photoreceptors from cell death in a mouse model of age-related macular degeneration. Cell death & disease 13(3): 255.
10. Nebbioso M, Franzone F, Greco A, Gharbiya M, Bonfiglio V, et al. (2021) Recent Advances and Disputes About Curcumin in Retinal Diseases. Clinical ophthalmology 15: 2553-2571.
11. Chakravarthy U, Peto T (2020) Current Perspective on Age-Related Macular Degeneration. Jama 324(8): 794-795.
12. Li JQ, Welchowski T, Schmid M, Mauschitz MM, Holz FG, et al. (2020) Prevalence and incidence of age-related macular degeneration in

Europe: a systematic review and meta-analysis. The British journal of ophthalmology 104(8): 1077-1084.

13. Wong WL, Su X, Li X, Cheung CM, Klein R, et al. (2014) Global prevalence of age-related macular degeneration and disease burden projection for 2020 and 2040: a systematic review and meta-analysis. The Lancet Global health 2(2): e106-16.

14. Zhao T, Guo X, Sun Y (2021) Iron Accumulation and Lipid Peroxidation in the Aging Retina: Implication of Ferroptosis in Age-Related Macular Degeneration. Aging and disease 12(2): 529-551.

15. Toma C, De Cillà S, Palumbo A, Garhwal DP, Grossini E (2021) Oxidative and Nitrosative Stress in Age-Related Macular Degeneration: A Review of Their Role in Different Stages of Disease. Antioxidants (Basel, Switzerland) 10(5): 653.

16. Shughoury A, Sevgi DD, Ciulla TA (2022) Molecular Genetic Mechanisms in Age-Related Macular Degeneration. Genes 13(7): 1233.

17. Schultz R, Gamage K, Messinger JD, Curcio CA, Hammer M (2020) Fluorescence Lifetimes and Spectra of RPE and Sub-RPE Deposits in Histology of Control and AMD Eyes. Investigative ophthalmology & visual science 61(11): 9.

18. Coronado BNL, da Cunha FBS, de Oliveira RM, Nóbrega OT, Ricart CAO, et al. (2021) Novel Possible Protein Targets in Neovascular Age-Related Macular Degeneration: A Pilot Study Experiment. Frontiers in medicine 8: 692272.

19. Ren J, Ren A, Deng X, Huang Z, Jiang Z, et al. (2022) Long-Chain Polyunsaturated Fatty Acids and Their Metabolites Regulate Inflammation in Age-Related Macular Degeneration. Journal of inflammation research 15(1): 865-880.

20. You L, Peng H, Liu J, Cai M, Wu H, et al. (2021) Catalpol Protects ARPE-19 Cells against Oxidative Stress via Activation of the Keap1/Nrf2/ARE Pathway Cells ;10(10): 2635.

21. Alhasani RH, Biswas L, Tohari AM, Zhou X, Reilly J, et al. (2018) Gypenosides protect retinal pigment epithelium cells from oxidative stress. Food and chemical toxicology: an international journal published for the British Industrial Biological Research Association 112: 76-85.

22. Li S, Jiang Y, Xing X, Lin R, Li Q, et al. (2021) Protective Mechanism of Berberine on Human Retinal Pigment Epithelial Cells against Apoptosis Induced by Hydrogen Peroxide via the Stimulation of Autophagy. Oxidative medicine and cellular longevity 7654143.

23. Pike ST, Rajendra R, Artzt K, Appling DR (2010) Mitochondrial C1-tetrahydrofolate synthase (MTHFD1L) supports the flow of mitochondrial one-carbon units into the methyl cycle in embryos. The Journal of biological chemistry 285(7): 4612-4620.

24. Sy C, Gleize B, Dangles O, Landrier JF, Veyrat CC, et al. (2012) Effects of physicochemical properties of carotenoids on their bioaccessibility, intestinal cell uptake, and blood and tissue concentrations. Molecular nutrition & food research 56(9):1385-1397.

25. Lee D, Xu IM, Chiu DK, Lai RK, Tse AP, et al. (2017) Folate cycle enzyme MTHFD1L confers metabolic advantages in hepatocellular carcinoma. The Journal of clinical investigation 127(5): 1856-1872.

26. Li H, Fu X, Yao F, Tian T, Wang C, et al. (2019) MTHFD1L-Mediated Redox Homeostasis Promotes Tumor Progression in Tongue Squamous Cell Carcinoma. Frontiers in oncology 9(1): 1278.

27. Huang DR, Dai CM, Li SY, Li XF (2021) Obacunone protects retinal pigment epithelium cells from ultra-violet radiation-induced oxidative injury. Aging 13(8): 11010-11025.

28. Billsten HH, Bhosale P, Yemelyanov A, Bernstein PS, Polívka T (2003) Photophysical properties of xanthophylls in carotenoproteins from human retinas. Photochemistry and photobiology 78(2): 138-145.

29. Green-Gomez M, Prado-Cabrero A, Moran R, Power T, Gómez-Mascaraque LG, et al. (2020) The Impact of Formulation on Lutein, Zeaxanthin, and meso-Zeaxanthin Bioavailability: A Randomised Double-Blind Placebo-Controlled Study. Antioxidants (Basel, Switzerland) 9(8): 767.

30. Garcia-Garcia J, Usategui-Martin R, Sanabria MR, Fernandez-Perez E, Telleria JJ, et al. (2022) Pathophysiology of Age-Related Macular Degeneration: Implications for Treatment. Ophthalmic research 65(6): 615-636.

31. Obana A, Gohto Y, Nakazawa R, Moriyama T, Gellermann W, et al. (2020) Effect of an antioxidant supplement containing high dose lutein and zeaxanthin on macular pigment and skin carotenoid levels. Scientific reports 10(1): 10262.

32. Xiao H, Wang J, Barwick SR, Yoon Y, Smith SB (2022) Effect of long-term chronic hyperhomocysteinemia on retinal structure and function in the cystathionine-β-synthase mutant mouse. Experimental eye research 214:108894.

33. Muralimanoharan S, Kwak YT, Mendelson CR (2018) Redox-Sensitive Transcription Factor NRF2 Enhances Trophoblast Differentiation via Induction of miR-1246 and Aromatase. Endocrinology 159(5): 2022-2033.

34. Sial N, Rehman JU, Saeed S, Ahmad M, Hameed Y, et al. (2022) Integrative analysis reveals methylenetetrahydrofolate dehydrogenase 1-like as an independent shared diagnostic and prognostic biomarker in five different human cancers. Bioscience reports 42(1).

35. Wu DM, Ji X, Ivanchenko MV, Chung M, Piper M, et al. (2021) Nrf2 overexpression rescues the RPE in mouse models of retinitis pigmentosa. JCI insight 6(2): e145029.

36. Zhao W, Zhang B, Liang W, Liu X, Zheng J, et al. (2022) Lutein encapsulated in whey protein and citric acid potato starch ester: Construction and characterization of microcapsules. International journal of biological macromolecules 220(1): 1-12.